

Minerals Dissolution Effect on the Mechanical Properties of Synthetic Carbonatic Rocks under a Reactive Fluid Injection

Katia Galindo^{a*}, Leonardo Guimarães^b, Cecília Lins^c, Analice Lima^d, Yago Santos^e, Igor Gomes^f

^{a,b,d,e,f}*Federal University of Pernambuco, Recife, Pernambuco, Brazil*

^c*Rural Federal University of Pernambuco, Cabo de Santo Agostinho, Pernambuco, Brazil*

^a*Email: katia.galindo@ufpe.br, ^bEmail: Leonardo.guimaraes@ufpe.br, ^cEmail: Cecilia.lins@gmail.com,*

^d*Email: analice.amorim@ufpe.br, ^eEmail: gomes@ufpe.br, ^fEmail: yago_ryan@hotmail.com*

Abstract

This research aims to evaluate the change in the stiffness and shear strength of synthetic carbonate rocks submitted to a reactive injection fluid. Therefore, laboratory tests were carried out with two types of cemented carbonatic rock artificially produced. The synthetic rocks were subjected to physical characterization tests (mineralogy, computed tomography, porosity, etc.) and mechanical characterization (uniaxial compressive strength and Brazilian tests) before and after the dissolution process to assess any changes in the samples. The dissolution test was performed in a modified oedometer cell, which allowed for measurements of horizontal displacements. The loading and dissolution phases were conducted using water and an acid solution to evaluate the influence of pH on their initial characteristics of the samples. The X-ray diffraction analysis revealed that the increase in maximum porosity by 57.8% and the increase in permeability were due to the dissolution of minerals. During dissolution, the horizontal stress increased linearly, and the maximum volumetric strain was 12.8%, owing to the loss of mass. This was also reflected in the mechanical characteristics since the samples lost about 72% of the strength after the dissolution with the acid solution. The study carried out in this paper helps explain and estimate changes on a micro-scale, that is, to understand how the dissolution of bonds between grains leads to macro-scale changes, such as the loss of mechanical strength causing irreversible damage to the rock.

Keywords: Synthetic carbonate rock; water-weakening; rock-fluid interaction.

* Corresponding author.

1. Introduction

Chemical weathering and fluid-injection and extraction processes modify the properties of rocks, including porosity, permeability, constituent minerals, and mechanical properties, which can generate problems that affect various applications in engineering which can cause change the built and natural environment and, consequently, prevent the sustainable exploration of geographic resources. The rock–fluid interactions can cause dissolution processes, inducing the matrix rock to weaken, which leads to deformation. Rock chemical compaction, for instance, results from the dissolution of the diagenetic bonds (between the grains), progressive grain size reduction, and pore collapse; the rock experiences grain redistribution, cementation, and change in the fluid flow dynamics. All the processes involved depend mainly on the reactivity of the fluid due to temperature and pressure, which can induce a complex interaction of multiphase flow, diffusion, convection, dissolution, precipitation, and other chemical reactions. The physical and mechanical properties of the rock are needed to assess the rock's stress states and to determine the various fluid properties in the porous medium, including quantity, distribution, movement behavior, and the amount that can be extracted ([1,2,3]). As an example, these interactions can generate a water-weakening effect, which can result in deformations that affect the mechanical behavior of the rock, such as decreasing strength and stiffness when subjected to various loads. This can cause compaction and subsidence of the rock, pressure buildup, collapsed wells, or a reduction of shear stresses in the well wall. The stress reduction can reactivate geological faults, inducing seismic events and, in some cases, collapse underground reservoir cavities. These phenomena can cause damage to the rock and, consequently, prevent the sustainable exploitation of natural resources [4,5,6,7,8]. In this context, the engineering field needs to understand the geomechanical and geochemical processes that occur in carbonate rocks, which are unstable to temperature and pressure and chemically reactive. The dissolution processes in these rocks often cause the removal of shells and other fragments in their structure and increased porosity. Later, these voids can be filled by cementation [9], presenting heterogeneous geomorphological characteristics. Because of the complexity of the phenomena involving carbonate rocks, their characterization, and the rock–fluid interactions, several studies have been conducted with synthetic rocks [10,11,12,13,14,15,16]. These investigations aimed to better control the physical and mechanical properties of rock and characterize its behavior through the simulation of the natural matrix of synthetic carbonate rock, using the main lithification factors, which, according to [16], include grain size and shape, the concentration of cementing material, and compaction pressure. For example, Reference [17] used fragments of natural limestone, Portland cement, and water for the production of synthetic rocks to perform mechanical tests and numerical simulations. Reference [14] used these same materials to produce synthetic carbonate rocks to study the influence of the rock's interaction with an acid fluid through the dissolution test, evaluating changes in the permeability and mechanical strength of the samples. The results achieved were, in the permeability and porosity decrease and UCS increase were probably due to pore throat obstruction phenomena, the formation of a stable layer on the reactive surface resulting from the cement dissolution and the supersaturation of Ca^{+2} cations causing precipitation. The constructed geochemical model represented harder dissolution at the system input and the precipitation caused by the dispersion from the reactive transport at the output. Reference [16] produced synthetic carbonate rocks composed of sand, calcite, and Portland cement. They studied the influence of the percentage of cement on the strength of the samples. A comparison was also made with the natural matrix of carbonate rocks about the main factors of lithification,

such as grain size and shape, the concentration of cementation material, and compaction pressure. The results were compared with natural carbonate samples and showed a high similarity to the petrophysical behavior of mudstones rocks. That similarity points out the feasibility of those synthetic rocks to be used as analogous of mudstones, specifically those exhibiting only primary porosity, in experiments regarding rock physics, core flooding or rock mechanics. Reference [18] used synthetic carbonates to study the behavior of compaction under conditions that favor the dissolution of grains under pressure. The authors investigated the effects of grain size and distribution, the behavior of compaction stress, and the effects of different fluid compositions, using theoretical models of dissolution under pressure. The experimental results suggest the main deformation mechanism in calcite under their experimental conditions was pressure solution and that diffusion is likely to be the rate-controlling process pure solution system. These studies involving synthetic rocks report the value of reproducing rocks in the laboratory, which result in samples with predetermined characteristics that can be used to develop correlations between their physical properties in laboratory tests and numerical simulations. According to [19], these synthetic rocks can be applied in engineering is to analyze the behavior of sandstones and soft carbonate rocks susceptible to compaction and subsidence. The objective of this paper is to evaluate the impact of chemical interactions between synthetic carbonate rocks and a reactive fluid and to analyze the linked hydraulic, mechanical, and chemical phenomena that can alter the initial characteristics of the rock. The paper aims to contribute to the understanding of rock behavior when subjected to reactive fluid injection. Two artificially cemented rocks were produced for this study— (1) with Portland cement and (2) with calcium hydroxide ($\text{Ca}(\text{OH})_2$) and carbon dioxide (CO_2). Physical and mechanical tests for rock characterization and dissolution tests under oedometer conditions were conducted. The dissolution test employed a modified oedometer cell specially designed to measure horizontal stress. For both studied samples, changes in the stress states and physical and mechanical properties that occur after these rocks were subjected to the reactive fluid are presented.

2. Testes protocols

Two types of artificially cemented carbonate rocks were studied. Then, dissolution tests were performed on the samples using a modified oedometer cell to obtain parameters of horizontal stress, volumetric strain, permeability, and pH during the test and to analyze physical parameters, such as mineralogy, porosity, void index, and grain density of the sample, before and after the test. Unconfined compressive strength (UCS) and diametral compression tests were performed to evaluate and compare the shear and tensile strengths, respectively, of the samples before and after the dissolution test. The methodology for sample production in the laboratory was standard for all samples— to obtain rocks with similar physical and mechanical properties, thus allowing for valid sample comparisons before and after the test.

2.1 Synthetic Carbonatic Rocks Production

The synthetic samples produced for this study comprised sand, calcite, and bonding material, with one sample artificially cemented with $\text{Ca}(\text{OH})_2$ reacting with CO_2 and the other with Portland cement, using the methodologies adapted from [20,14], respectively. This composition was based on the sedimentary formation of soft carbonate rocks that predominantly consist of bonded limestone fragments (ooids, shells, and corals).

Additional composition information was obtained from tests carried out with natural carbonate rocks, comprising mainly calcite/dolomite/aragonite and secondary minerals, such as anhydrite, gypsum, siderite, quartz, clay minerals, pyrite, oxides, and sulfates [2,21,6,14]. Table 1 shows the percentages of materials that were used in the samples.

Table 1: Percentages of materials used in synthetic rocks.

Agglomerate	Fraction (%)				
	Calcite	Sand	Lime	Cement	Water
With calcium hydroxide + CO ₂	25	50	25	-	20
With Portland cement	68	3,6	-	28	20

*Methodology adapted from [20].

** Methodology adapted from [14].

The dry mass of calcite and sand was washed and sieved to a granulometric fraction of 0.50 mm, then divided, and each part was mixed with a cement—(a) Ca(OH)₂ + CO₂ (abbreviated as CH) and (b) Ari Portland (CP V-ARI) cement and water (CC). The percentage of water was based on the weight of the aggregate mixture (agglomerate, sand, and calcite). The components were mixed manually for 5 min to obtain a homogeneous mass. Then, the mixture was uniformly poured in a steel compaction mold, where static compaction was performed in a servo-controlled press, exposed to vertical stress of 15 MPa. For the CH sample, the compacted mixture in the compaction cell was then exposed to direct carbonation with a pressure of 100 kPa of CO₂ for 5 min and placed in a drying oven at 105°C for 24 h. For the CC sample, the mixture remained in the press for 12 h with the applied compression stress and was then taken to the muffle for 32 h with a temperature range of 100 to 300°C. After the cementation procedures, the samples were extracted from the molds for the test protocols (Figure 1).

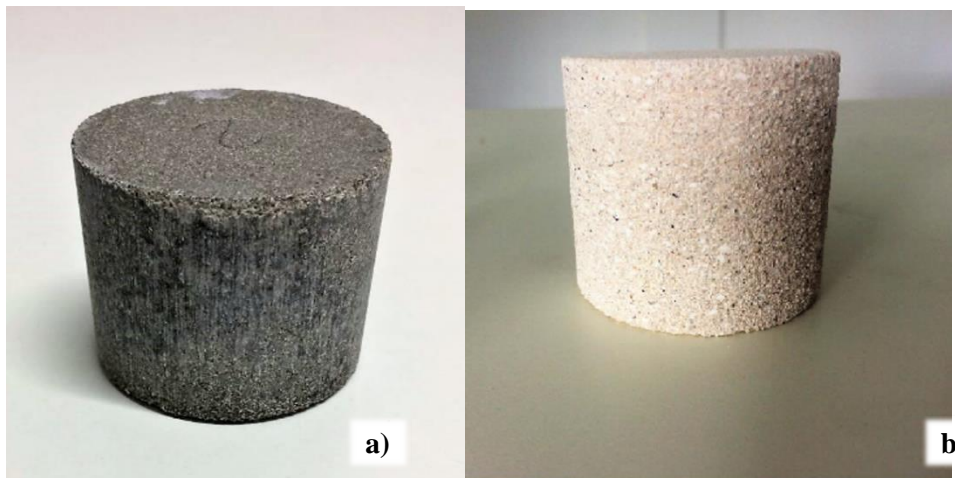


Figure 1: Samples after mold extraction. a) With Portland cement; b) With calcium hydroxide.

2.2 Dissolution Test under Oedometer Conditions

The modified oedometer cell in this study, which was developed by [22], is made of a bronze-aluminum alloy and has a containment ring with a 7.0-cm diameter, 6.5-cm height, and 0.8-mm thickness. The cell was designed to measure radial strain on a millimeter scale and its consequent horizontal stresses, as shown in Figure 2. High-resolution strain gauges were installed in the oedometric cell ring to collect radial data and for LVDT (displacement transducer) vertical displacement measurements. After the instrumentation, the rock sample was put into the modified oedometric cell, which was then placed in the loading frame. The LVDT was calibrated, and the LVDT and extensometers were connected to a computer to feed the software Geolab the stress and strain data. For the injection of the reactive fluid, a reservoir was installed next to the loading frame, as shown in Figure 3.

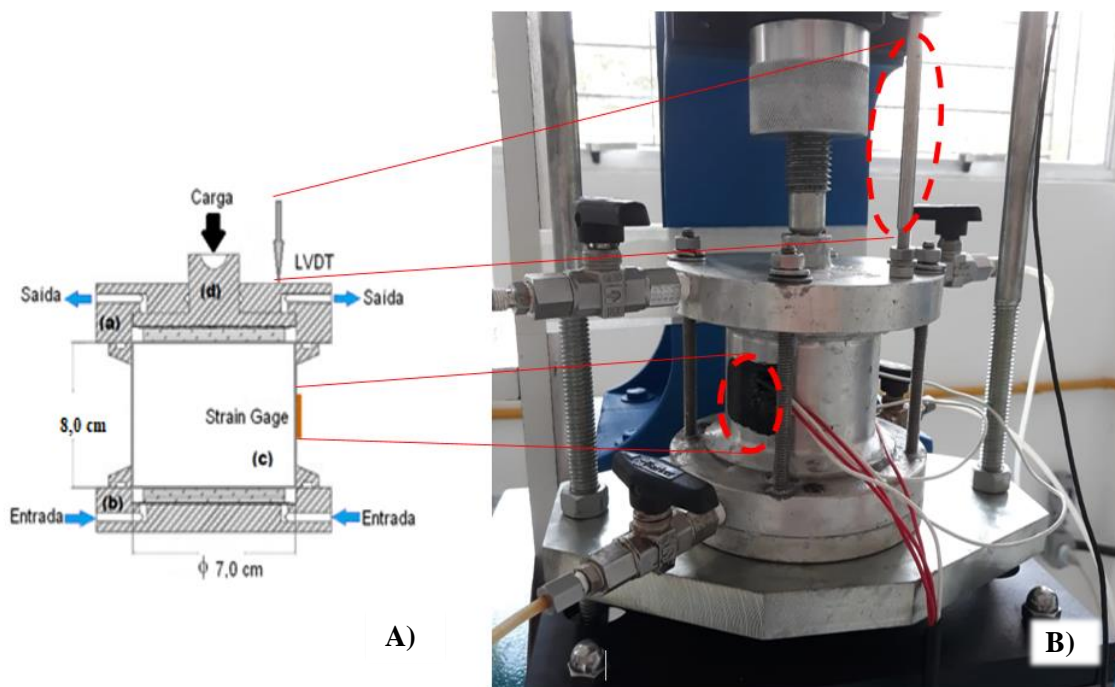


Figure 2: A) Scheme of the oedometer cell with chemical weathering composed of: (a) top, (b) bottom, (c) confining ring, e (d) piston for vertical load. B) Modified oedometer cell, with focus on the extensometer in the confining ring and the LVDT in the upper part of the cell. **Reference: [22] Modified.**

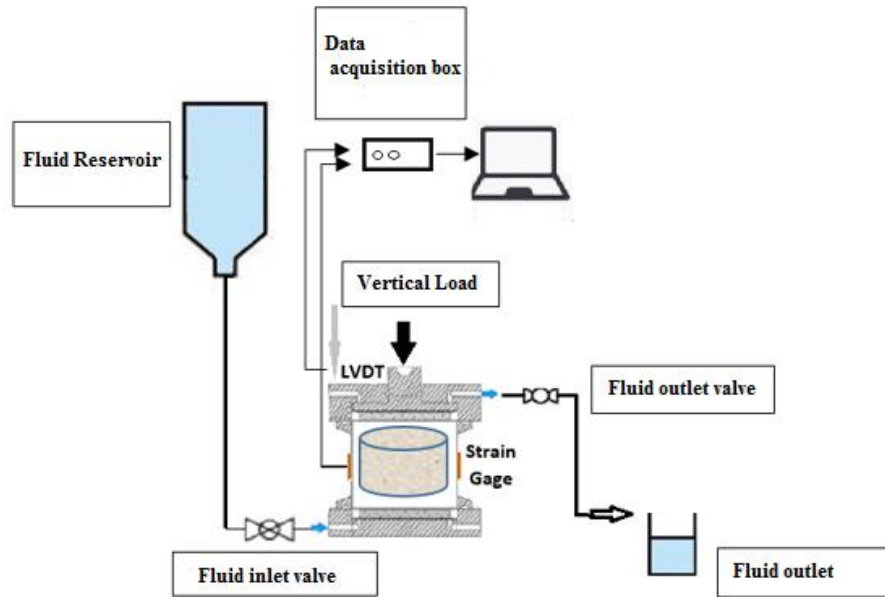


Figure 3: Scheme of the experimental apparatus of the dissolution test.

For the dissolution test, two types of fluids were used water and acetic acid solution (with 10% concentration)—with their characteristics described in Table 2. The fluid was injected upwards, as illustrated in Figure 2(a).

Table 2: Fluid specifications used in dissolution test.

Fluid	Water	Acetic acid
Viscosity	0.89 mPa.s	1.22 mPa.s
pH	7.0	2.8
Density	1.0 g/cm ³	1.049 g/cm ³
Chemical formula	H ₂ O	C ₂ H ₄ O ₂

Based on the literature, protocols have been defined to subject the rocks to conditions of pressure and fluid exposure. The following list of protocols describes the different methodologies used for the dissolution tests: Protocol 1: This methodology consists of the loading and dissolution phases. In the loading phase, vertical loads of 150, 300, and 400 kPa are applied for 1 h each (tree specimen per applied load). Then, dissolution starts with the acetic acid solution at a flow pressure of 2 kPa for approximately 7 h, totaling 15 injected through the synthetic rock. During the test, pH, permeability, and vertical and horizontal displacements are measured. The acid solution is collected for every 200 ml of percolating fluid to measure the pH with the pH meter. This methodology was carried out on the two samples of synthetic rock. Protocol 2: The difference between this methodology and the previous one can be observed in the dissolution phase, where acetic acid is applied with a flow pressure of 12 kPa for approximately 7 h, followed by 12kPa of acid and water for 12h. This methodology was carried out on both samples types of synthetic rock. Protocol 3: In this methodology, the loading and dissolution phases are interspersed. The loading phase is divided into two steps: (a) loading 1, followed by dissolution with the acetic acid solution, and loading 2, followed by dissolution with water, and (b) dissolution

with acid for 2 h and then with water for 10 h. This methodology was carried out on the CC rock sample. On the microstructural level, the dissolution causes the degradation of bondings between the solid grains of the rock. These different dissolution protocols were carried out to evaluate the interaction between the fluid and the synthetic rock under different contact time and pressure conditions. Higher vertical loads were not applied as the oedometer cell was calibrated up to 400 kPa.

2.3 Evaluation of the effect of dissolution on the physical and mechanical properties of rocks

2.3.1 Physical characterization of synthetic rock samples

The synthetic carbonate rocks were characterized by determining their physical properties, such as porosity, void index, particle density, grain-size distribution of the mixture, mineralogy through the X-ray diffraction, tomography (analyzed by the CT equipment of the LTC-RX), and petrography (analyzed using a scanning electron microscope (SEM) Nikon Eclipse Pol). These measurements were performed before and after the reactive fluid injection.

2.3.2 Mechanical tests—unconfined compressive strength and Brazilian tests

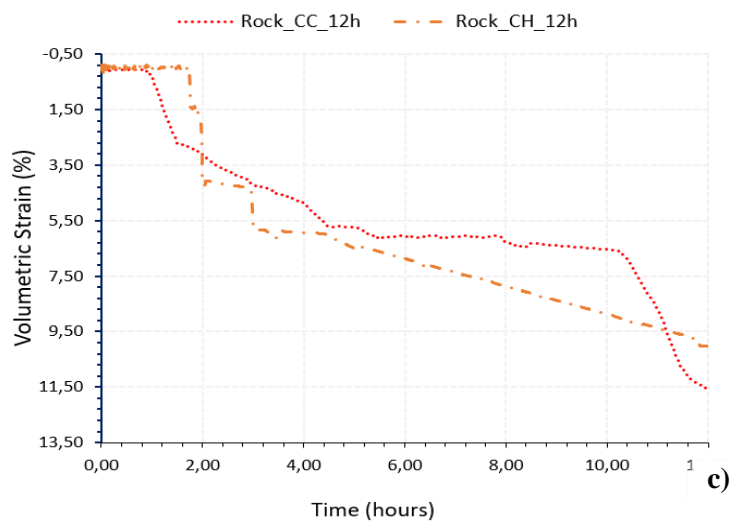
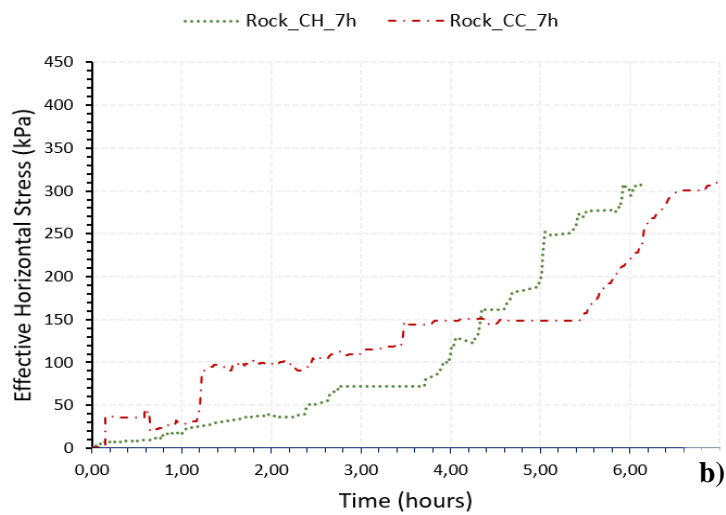
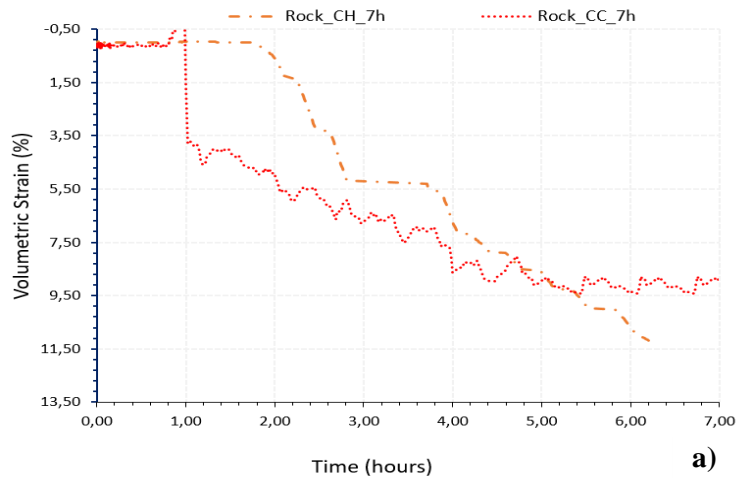
UCS tests were performed to determine the maximum strength and Young's modulus (E) of the synthetic carbonate rocks. The dimensions of the test samples were 65 mm long by 33 mm in diameter. The tests were executed in a servo-controlled press with a constant vertical displacement speed of 0.122 mm/min. Fragile rocks require a speed of 0.4 mm/min, as recommended by the standard [23]. For synthetic rock, the lowest speed of the press was used. In the Brazilian test, the tensile strengths of samples with dimensions of 13 mm in height and 30 mm in diameter were measured. This value was based on the maximum stress that the specimen could support without breaking, with the load applied along the cylindrical axis. The test was performed on the same servo-controlled press as the UCS test with a constant vertical displacement speed of 0.122 mm/min.

3. Experimental Results

3.1 Dissolution test under oedometer conditions

For this stage 39 trials were counted in total. Figure 4a shows the evolution of the volumetric strain in the dissolution test over time, carried out with the Protocol 1 methodology, in which the sample was exposed to an axial load for 1 h, followed by an injection of acid flow. Based on the figure, during the loading phase, the volumetric strain of the CH and CC rock samples remained constant. In the dissolution phase, the material weakened because of the dissolution of the calcite minerals from the acid flow. The material deformed vertically, and the effective horizontal stress gradually increased, as shown in Figure 4b. According to Lins and his colleagues (2015), this increase in the effective horizontal stress is directly related to the development of the horizontal plastic expansion strains when the sample was submitted to oedometer conditions. Figures 4c and 4d show the results of the evolution of the volumetric strain and effective horizontal stress over time, following Protocol 2. In this test, the sample was exposed to a higher pressure of the fluid flow and a longer dissolution time. In both the loading and dissolution phases, the behavior was similar to that of Protocol 1. However, the volumetric strain values are more significant. The volumetric strain was also evaluated in the samples of the

fluid flow with water (Figure 4e), and the obtained deformation is patently low.



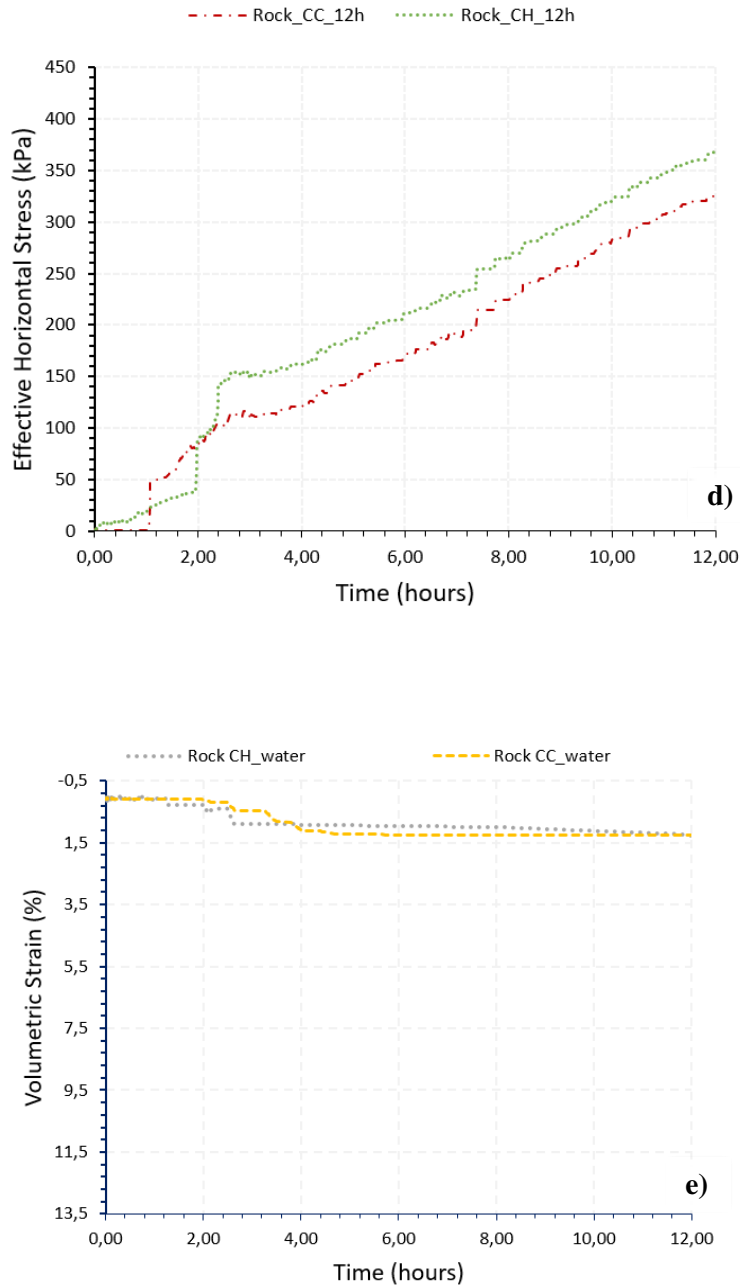


Figure 4: Results of the oedometer test with chemical degradation—a) and b) Protocol 1 dissolution (7h), c) and d) Protocol 2 dissolution (12h), and e) Protocol 2 dissolution (12h) with water for rock samples with cement (CC) and with calcium hydroxide (CH).

Mineral dissolution in the rocks caused an increase in the pH output value of the acid solution because calcium, when reacting with excess hydrogen, decreases the concentration of hydrogen ions (H⁺), increasing the pH solution. Figure 5 shows that the pH in the sample with calcium hydroxide increased from 2.8 to 4.5, and the pH of the CC sample increased from 3 to 4, indicating that a reaction occurred between the acid fluid injected and the synthetic rock samples. Even if the variations of the tests performed with water (pH = 7), both related to the effective horizontal stress, as well as the volumetric strain of tests performed with water, the minerals dissolve,

being identified in the comparison of pH input and output values of the fluid solution. Another change in the rock sample properties regarding this mineral loss during the fluid injection was in permeability. Throughout the test, the rock became more permeable, obtaining a final permeability coefficient close to 2.5 cm/s, as shown in Figure 6.

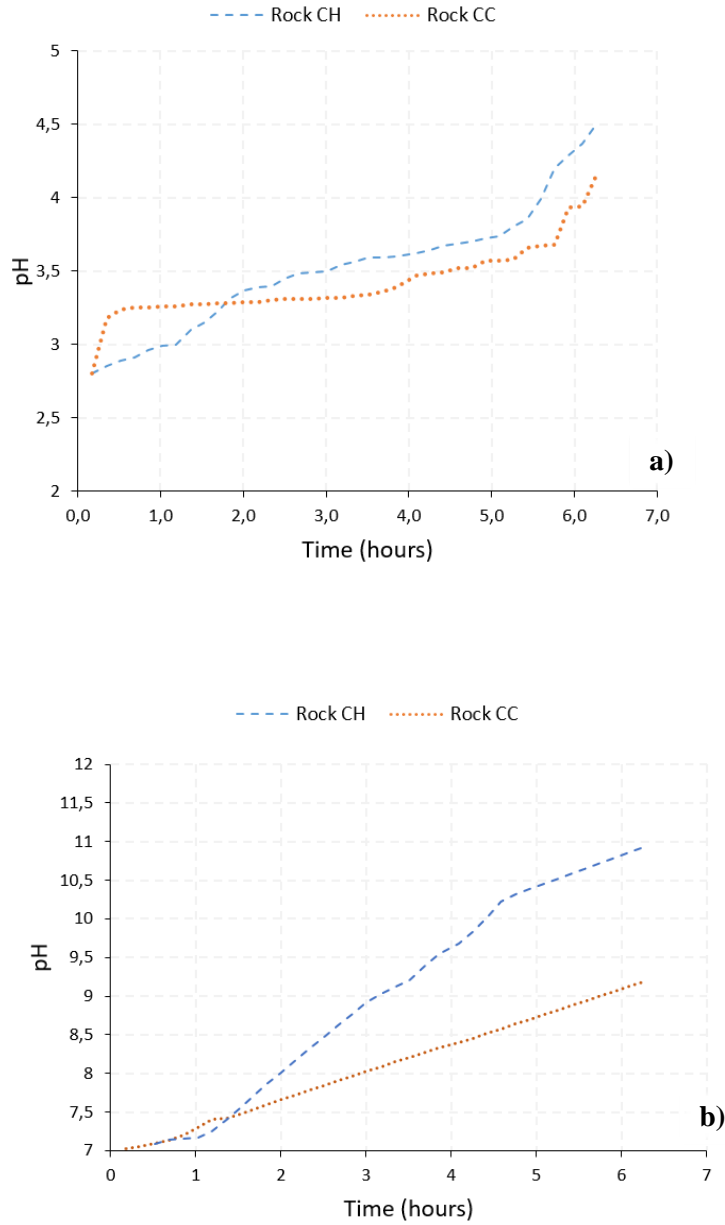


Figure 5: pH output values of the a) acid solution and b) water during dissolution.

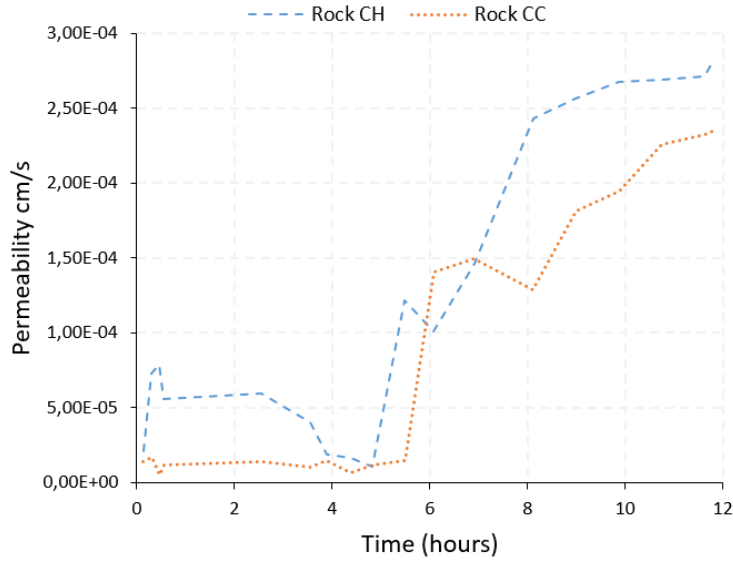


Figure 6: Rock permeability during dissolution.

Protocols 1 and 2 were carried out in two phases, loading (1–2) and dissolution (2–3), and the change in the state of stresses from one phase to another is represented in the plane $q-p'$ shown in Figure 7. This change is characterized by a decrease in the deviator stress q and compensated by an increase in the average stress p' from chemical degradation. Reference [10,22,6] also showed that the evolution of the stress path depends on the mechanical and chemical effects that occur simultaneously during the test. The CC rock was less degraded than the CH rock, corroborating the results of the volumetric strain.

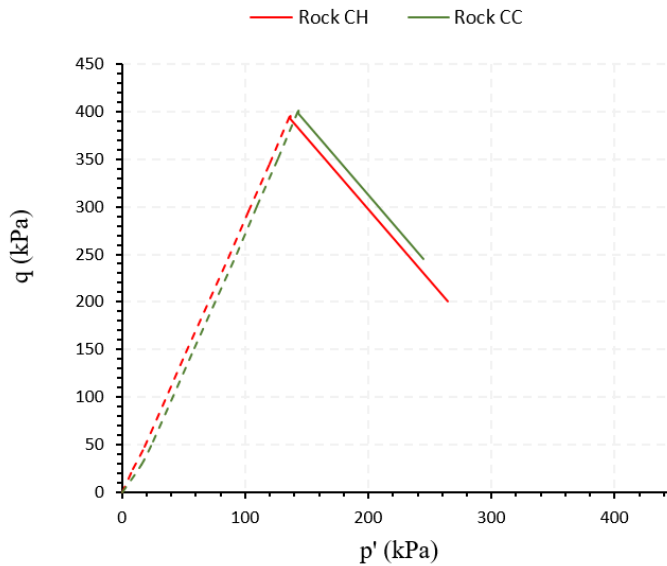


Figure 7: Stress path.

The results in Figure 6 and Figure 7 are needed to analyze the influence the weakening phase (sample softening) has on the mechanical behavior of the sample at different dissolution times because, as the rock loses its bondings, the elastic domain decreases, and the mechanical strength of the rock is affected. The tests with water (pH = 7) in Protocols 1 and 2 obtained much lower volumetric strains when compared to the acid fluid (Table 3); however, the higher applied load and longer dissolution time with the acid solution resulted in more sample degradation, corroborating with a study by [24]. These authors found that when a carbonate material is kept in contact with water for a long time (hours), the weakening of the solid structure is attributable to the chemical reaction of calcium carbonate dissolution. This dissolution is intensified with the acid, owing to physical and chemical factors that influence the solubility coefficient of calcium minerals in the rock. The results in Figure 8 were obtained by Protocol 3, where the loading and dissolution phases were interspersed, with acid as the first fluid injected into the cement rock, followed by water. Figure 7 shows the evolution of the volumetric strain over time, in which the sample reaches a maximum value of 9.4% after dissolution for 12 h. The dissolution with acid of 2 h yielded a maximum volumetric strain of 3.76 %, while 10 h with water resulted in a volumetric strain of 3.6%.

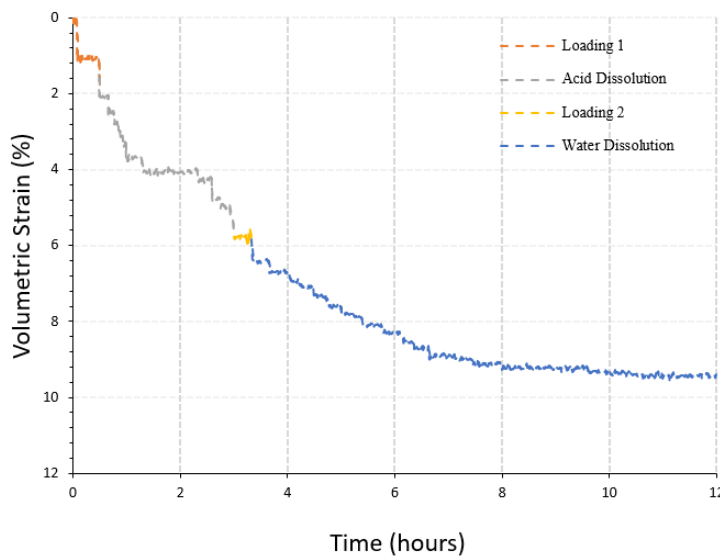


Figure 8: Volumetric strain of Protocol 3 dissolution with acid and water in the CC rock sample.

As shown in Figure 4e, the strain due to the dissolution with water is lower when compared to that with the acid flow. However, in Protocol 3, Figure 8 shows that the volumetric strain increased from 2.1% to 3.6% in the dissolution with acid, as the sample was submitted to a softening phase with the injection, thus, allowing the subsequent water injection to intensify in the dissolution process. In this methodology, only samples of rock with CP – V ARI were used. These processes can explain the behavior of rock when its stress state is modified once exposed to reactive fluids, which can affect the reservoir strain. Table 3 shows the results of maximum volumetric strain, horizontal stress, and dissolved mass index obtained in the dissolution test performed with water and acid. A total of 39 tests were performed; Table 3 shows the maximum average of three tests for each

vertical stress applied in each protocol.

Table 3: Maximum values obtained in each dissolution test.

Sample	Vertical Stress (kPa)	Horizontal Stress (kPa)	Strain (%)	Dissolved Mass Index
With Calcium Hydroxide	150 (Protocol 1)	20,253	9	13,78
	300 (Protocol 1)	102,073	10,66	15,84
	400 (Protocol 1)	307,980	11,43	15,95
	400 (Protocol 2) 7h	309,979	11,50	16,01
	400 (Protocol 2) 12h	439,543	12,75	18,23
400 (Protocol 2) H ₂ O 12h			1,6	2,1
With Portland Cement	150 (Protocol 1)	10,273	5,1	5,8
	300 (Protocol 1)	91,027	7,3	7,7
	400 (Protocol 1)		9,0	9,2
	400 (Protocol 2) 7h	300,002	9,5	9,2
	400 (Protocol 2) 12h	404,661	10,02	12,47
	400 (Protocol 2) H ₂ O 12h		1,2	1,6
	400 (Protocol 3) 12h		9,4	11,85

3.2 Dissolution effect on the physical and mechanical properties of rocks

The results of porosity, void index, grain density, tomographic images, and mineralogical analyses are presented along with the results of mechanical, compression, and tensile tests obtained before and after dissolution tests.

3.2.1 Physical indexes before and after degradation with acid solution

To quantify the degradation that occurred in the samples of synthetic rock in physical and mineralogical terms, analyses were performed before and after the dissolution tests with the acid solution, as shown in Table 4. The increase in physical indexes (porosity and void indexes) is a consequence of the carbonate mineral dissolution found in the samples of synthetic rocks, where the maximum increases in porosity achieved after the dissolution tests were roughly 44.3% for the CH sample and 61.2% for the CC sample. As a result, their unit weights decreased as well.

Table 4: Physical analysis of samples before and after Protocols 1 and 2.

Sample	Test	$\rho_g(g/cm^3)$	e	\emptyset (%)
With Calcium Hydroxide	Before Dissolution	1.60	0.577	35.78
	Protocol 1(7h)	1.50	1.200	54.00
	Protocol 2 (12h)	1.20	1.370	57.80
	Protocol 2 H ₂ O	1.60	0.560	35.67
With Portland Cement	Before Dissolution	1.70	0.580	36.80
	Protocol 1	1.50	0.900	47.40
	Protocol 2 (7h)	1.30	1.090	52.20
	Protocol 2 (12h)	1.25	1.130	53.10
	Protocol 2 H ₂ O	1.70	0.580	36.20

The mass loss, verified by the reduction of unit weight, is evidenced in the computed tomography (CT) images (Figure 9), where an increase of black pixels in the image (representing pores) is observed after the dissolution of cement samples. In the comparison of the two samples, including stress, strain, and porosity, the CH sample “suffers” more with dissolution than the CC sample. Therefore, the CT images indicate internal cracks appearing in the CH sample, in addition to the increase in pores as compared to CC. The CH sample contains a binding compound more willing to react compared to that of the CC sample; thus, the effects in the CH sample of dissolution were more significant.

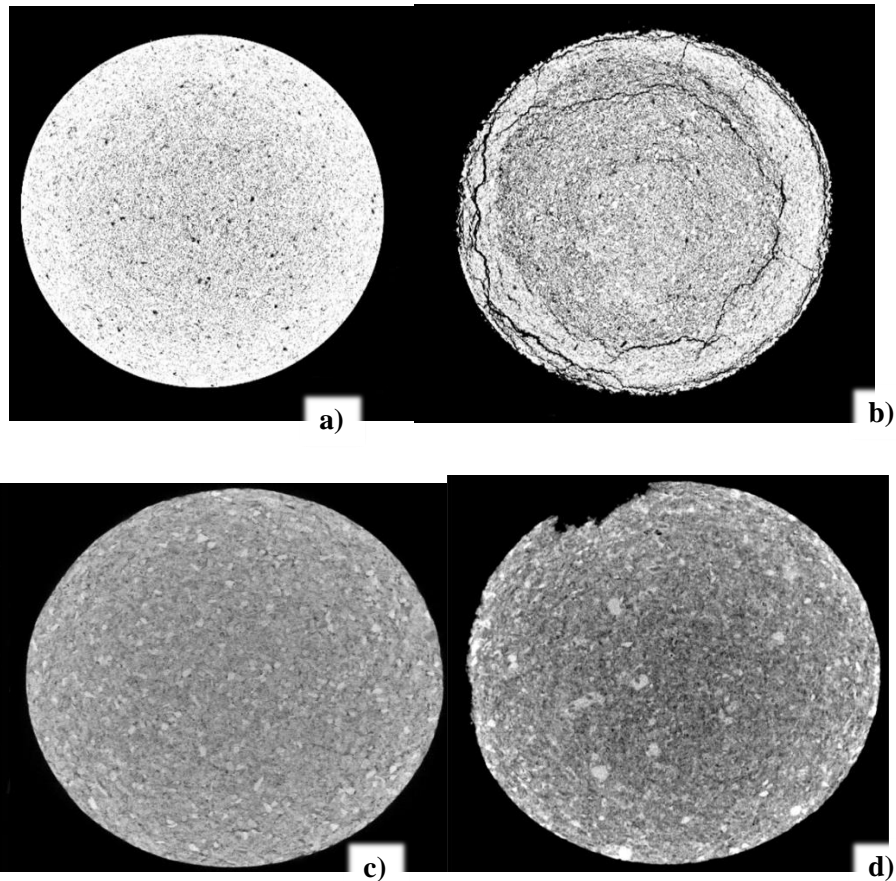


Figure 9: Tomography of samples (a) before CH dissolution, (b) after CH dissolution, (c) before CC dissolution and (d) after CC dissolution.

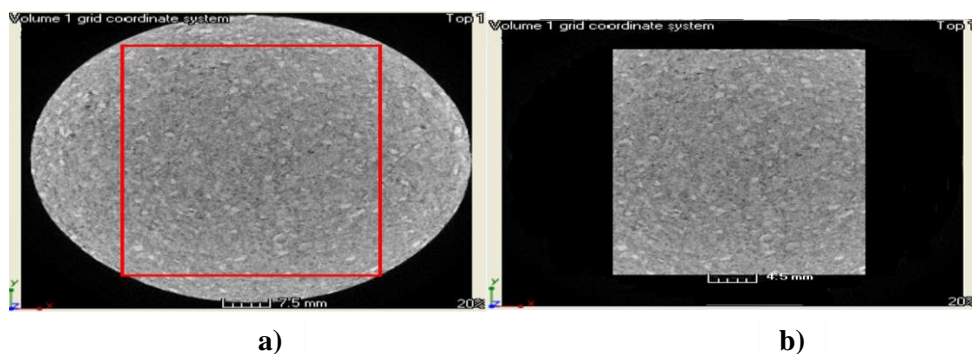


Figure 10: (a)CT image of slices of the entire sample, and (b) cut of the sample slices from the central zone.

When visualizing the spatial structure of the pores in the sample, a zone was selected in the middle of its main section to better quantify, analyze, and compare the microstructural changes attributed to the fluid flow (Figure 10).

From this central zone, a 3D construction of the pores in the sample was generated, showing their arrangement and number. After the rock–fluid interaction, the minerals dissolved, and, consequently, the pores increase in number and size. Figure 11 shows the studied volume of the samples, and Figure 12 indicates a considerable increase in the number of pores.

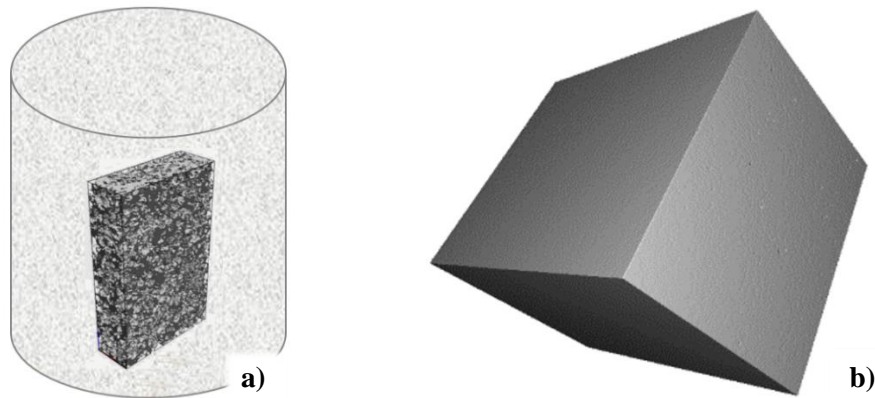


Figure 11: (a) Segmented 3D pore structure representation and (b) pore quantification study structure.

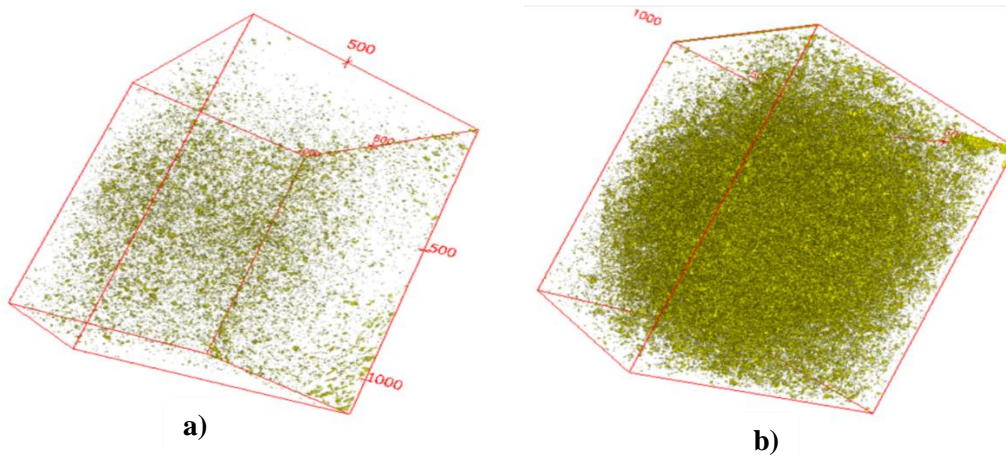


Figure 12: (a) 3D pore structure of the pre-dissolution sample and (b) 3D structure of the pores of the post-dissolution sample.

In the analysis of CT images, solids from non-solids and pores from non-pores can be differentiated. Therefore, sample data can be obtained for the quantification of small, medium, and large pores. Table 5 shows the porosity comparison obtained from CT images with the values acquired in the laboratory. The quantification analysis of the porosity through the reconstruction of the CT images is a non-destructive technique and takes into account

the absolute porosity of the samples; that is, it quantifies both the connected (permeable) and non-connected (closed) voids. The pore distribution analysis using the X-ray CT technique combined with 3D reconstruction was an effective tool to verify the increase in porosity both in terms of quantification in numerical percentage and the internal geometric structure of the pore rock samples.

Table 5: Porosity values comparison.

Method	Test	Ø (%)
Tomography	Before Dissolution	31,62
	After Dissolution	49,2
Laboratory	Before Dissolution	35,78
	After Dissolution	53,1

Table 6 shows how the quantification of the porosity distribution behaves according to the size of the analyzed particles. The size of the image takes into account the quality (number of pixels x, y) and the number of slices analyzed z. With the dissolution that occurred in the samples, the distribution of the pores is indicated by the size of the particles. Large pores are more representative after the dissolution, implying the grains susceptible to dissolution are dissolved and an increase of both existing and new pores occurred.

Table 6: Behavior of the porosity distribution by particle size.

Samples	Pores Distribution (%)			
	Image Dimension (x, y, z)	Small Pores	Medium Pores	Large Pores
CC Before Dissolution	(948*1128*1311)	0,094	0,723	2,344
CC After Dissolution	(948*1128*1070)	0,0067	0,027	49,15

From a microscopic perspective, calcium carbonate polymorphs occur in hand samples as rounded, white grains of coarse-sand to silt granulation. Skeletal grains can be observed, such as gastropod shells, bivalves, sea urchin spikes, and fragments of the green algae group, identified as Halimeda. Quartz occurs as rounded grains, white to transparent in color, medium- to fine-sand granulation, and usually presents a surface film of iron oxide change around the grains, as shown in Figure 13 of the images acquired by Dino-Lite Pro magnifying glass.

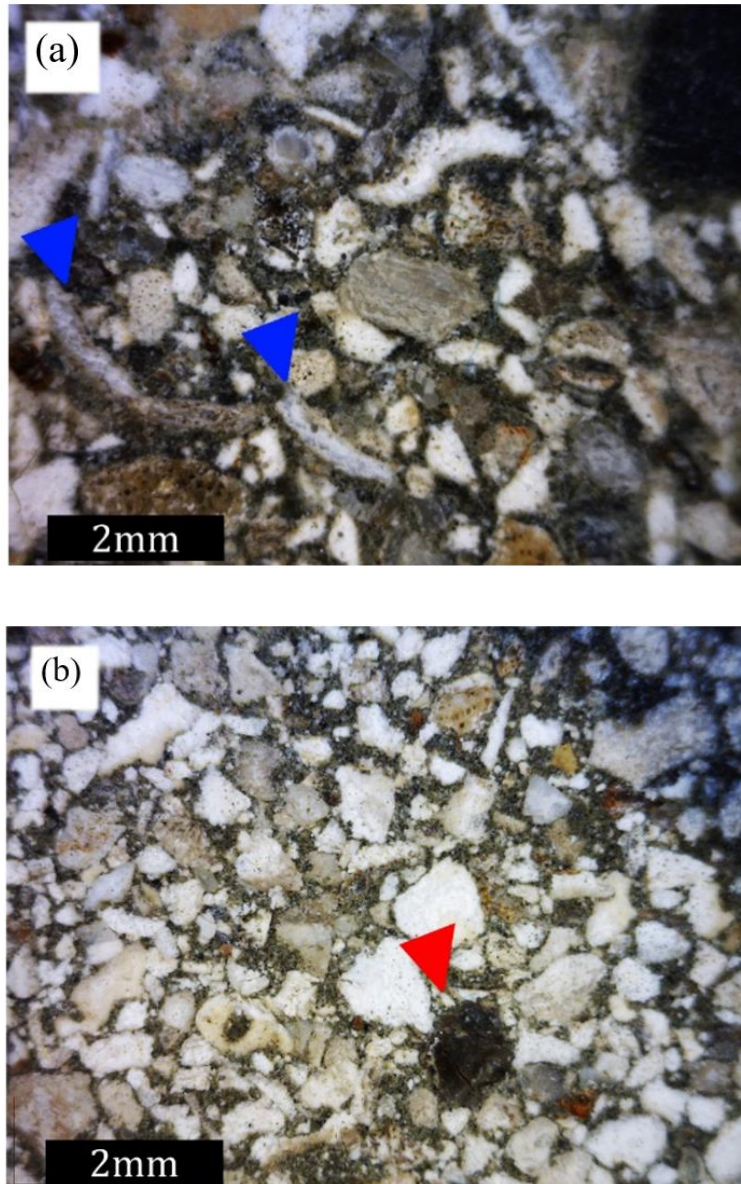


Figure 13: General aspects observed in the Dino-Lite Pro magnifying glass, (a) skeletal carbonate grains interpreted as bivalve carapaces (blue arrow) and (b) quartz grains covered with a superficial iron percolating film (red arrow).

The synthetic samples have a “primary” porosity associated with the voids inside the grain and between the grains. When comparing the aspects before and after dissolution, an increase of this primary porosity occurred after the passage of fluid through the synthetic rock due to the intergranular and intragranular voids and the creation of pores by dissolving the carbonate grains, as shown in Figure 14b (pores are represented in black) and Figure 15b (pores are blue and indicated by the green arrow). The carbonate grains in parallel nicols are yellowish to transparent white, and, under crossed nicols, they present a high interference color characteristic of the polymorphs of calcium carbonate, aragonite, and calcite [25]. Skeletal grains were also observed under the petrographic microscope, mainly fragments of the Halimeda, with their characteristic internal structure.

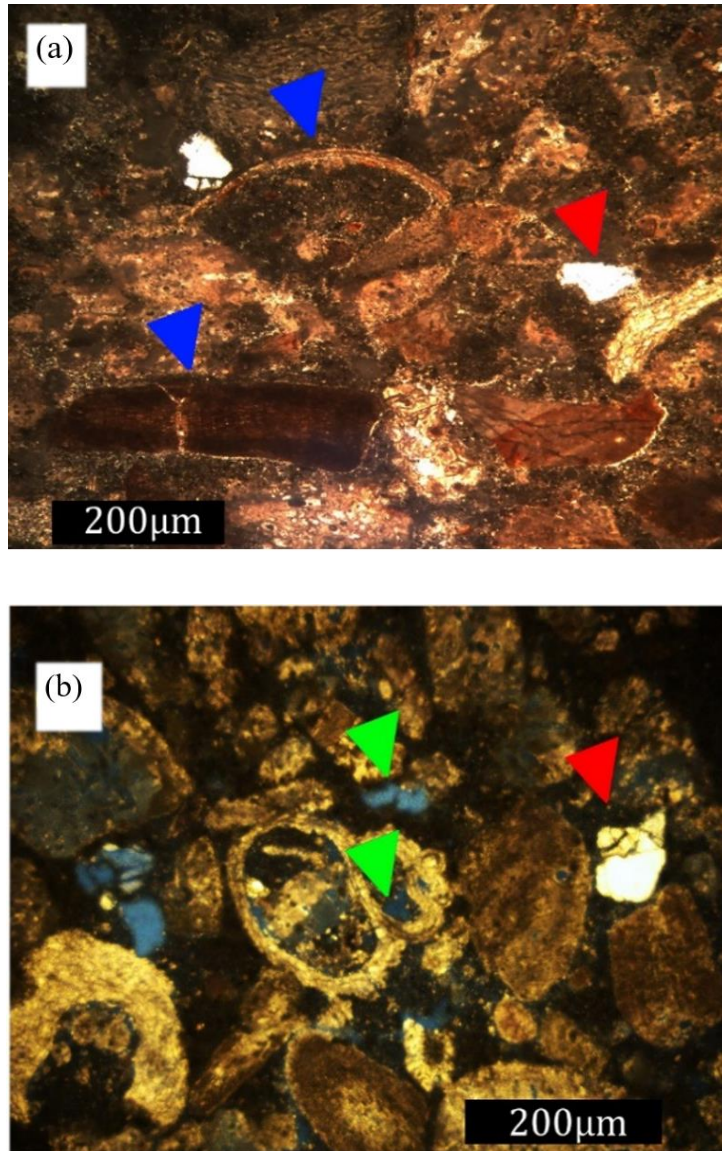


Figure 14: Micrograph obtained in the petrographic microscope (Nikon Eclipse Pol) with crossed nicols of the synthetic carbonate rock (a) before and (b) after dissolution—(a) detail for the Halimeda green algae fragment (lower blue arrow), a bivalve shell (upper blue arrow), and faceted feldspar grain (red arrow), (b) porosity (green arrow) and rounded quartz grain (red arrow).

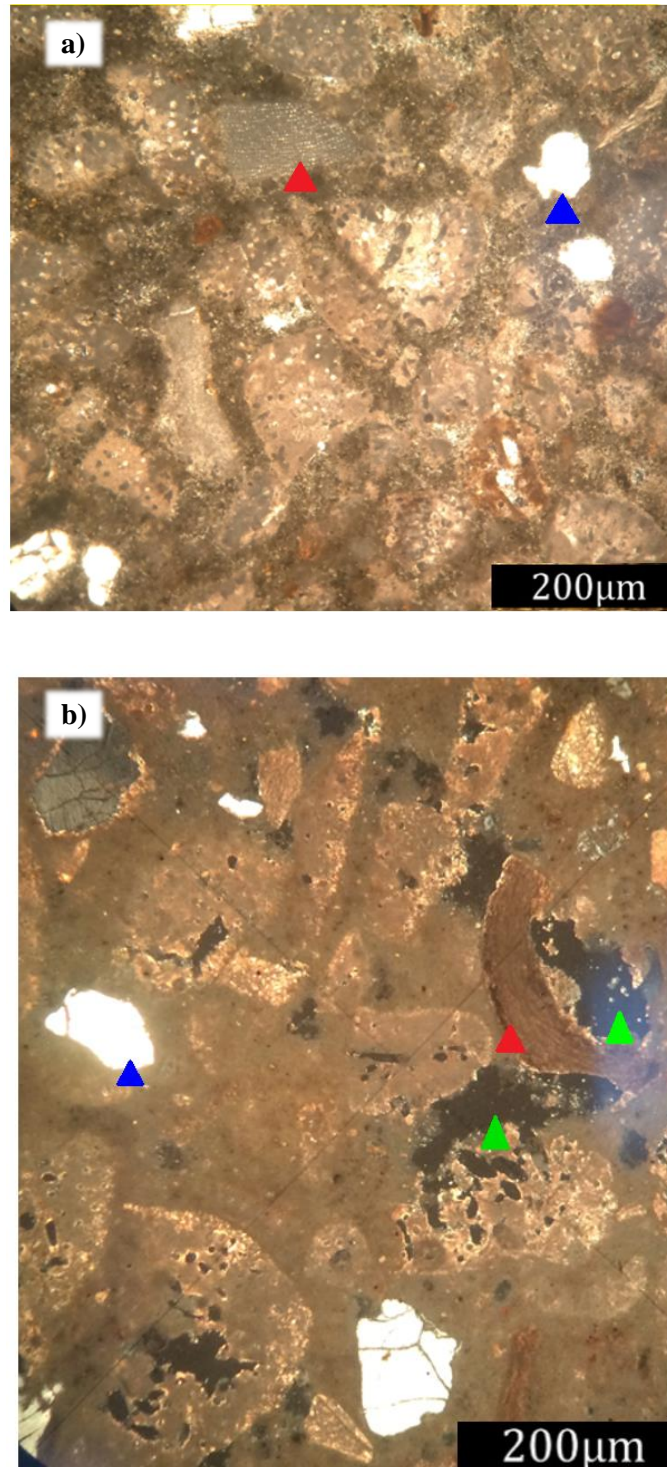


Figure 15: Micrograph obtained from the petrographic microscope (Nikon Eclipse Pol) to parallel nicols of the samples (a) before and (b) after dissolution. Skeletal grain of calcium carbonate from a gastropod (Blue arrow - carbonate skeletal grain; Green arrow - Porosity; Red arrow - quartz grain).

The appearance of intraparticle porosity was more evident in the dissolution of samples lasting 12 h, which can be better observed in Figure 16.

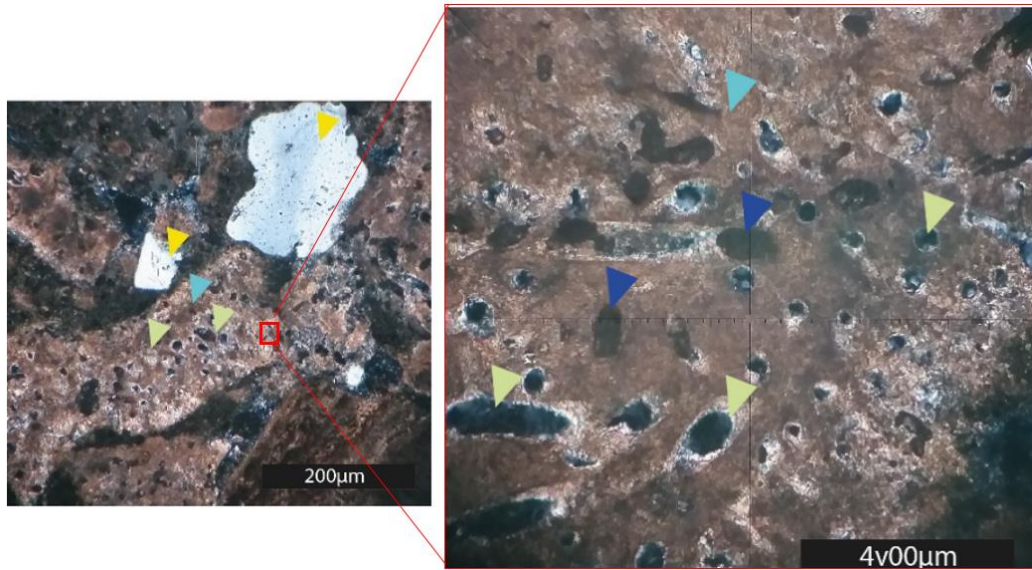
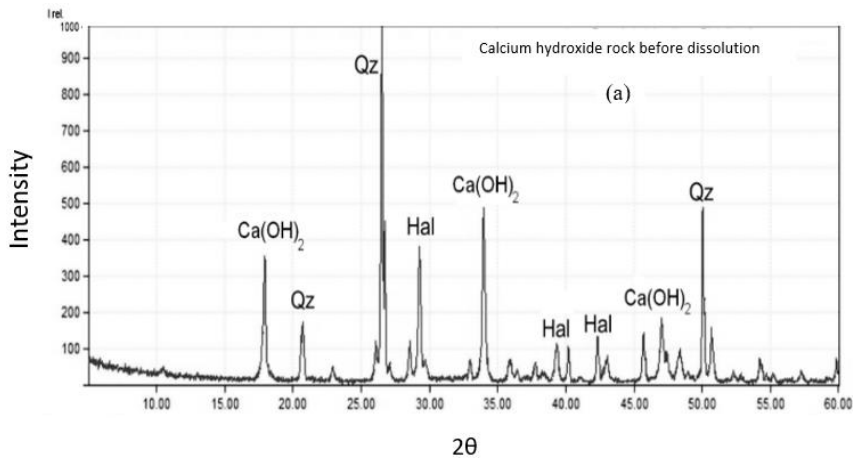


Figure 16: Images of the petrographic slide of the 12-h dissolution of the CC sample, with emphasis on the increase of intra-particle porosity. (Light green arrow - Intra-particle porosity; Light blue arrow - Halimeda; Yellow arrow - quartz grain; Blue arrow - Cement).

Figures 17 and 18 show the X-ray diffraction test with the 2θ angle graphs by the intensity of the diffracted peaks, and decreases in the Halimeda (Ca), calcium hydroxide, and aragonite (Ar) proportions are evident. Comparing the peak intensities of these minerals before and after the acid dissolution for the CH sample shows that $\text{Ca}(\text{OH})_2$ was more dissolved than Ca (Figure 17 a–b). In the CC sample, the Ca was more dissolved than Ar (Figure 18 a–b). The quartz mineral (Qz) presented an inert behavior to the fluid injected in both the CH and CC samples. The dissolution of carbonate minerals due to acid pH caused a decrease in the stability of the crystalline structure of calcium carbonate, favoring solubility. $\text{Ca}(\text{OH})_2$ has a higher solubility coefficient compared to Ca and Ar and, therefore, was the most dissolved, with solubility values at an ambient temperature of 0.185 g/l ($\text{Ca}(\text{OH})_2$), 0.0013 g/l (Ca), and 0.0014 g/l (Ar).



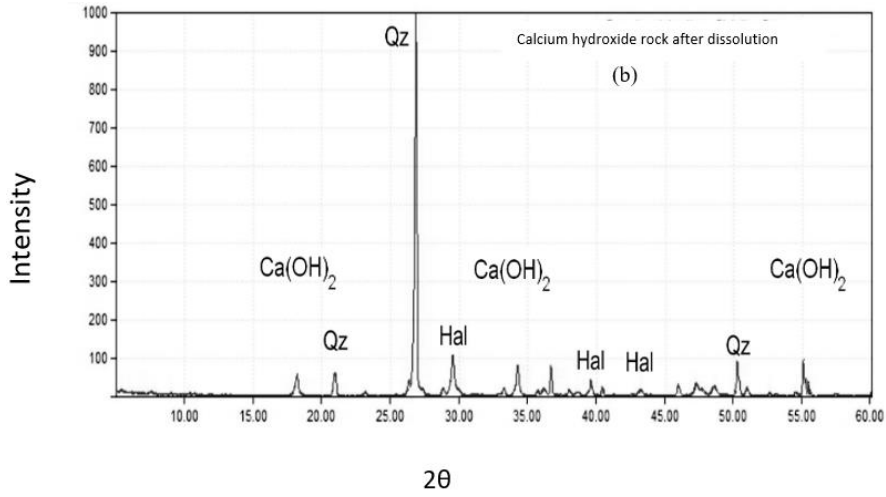


Figure 17: X-ray diffractogram of synthetic rock with calcium hydroxide (a) before dissolution and (b) after sample dissolution

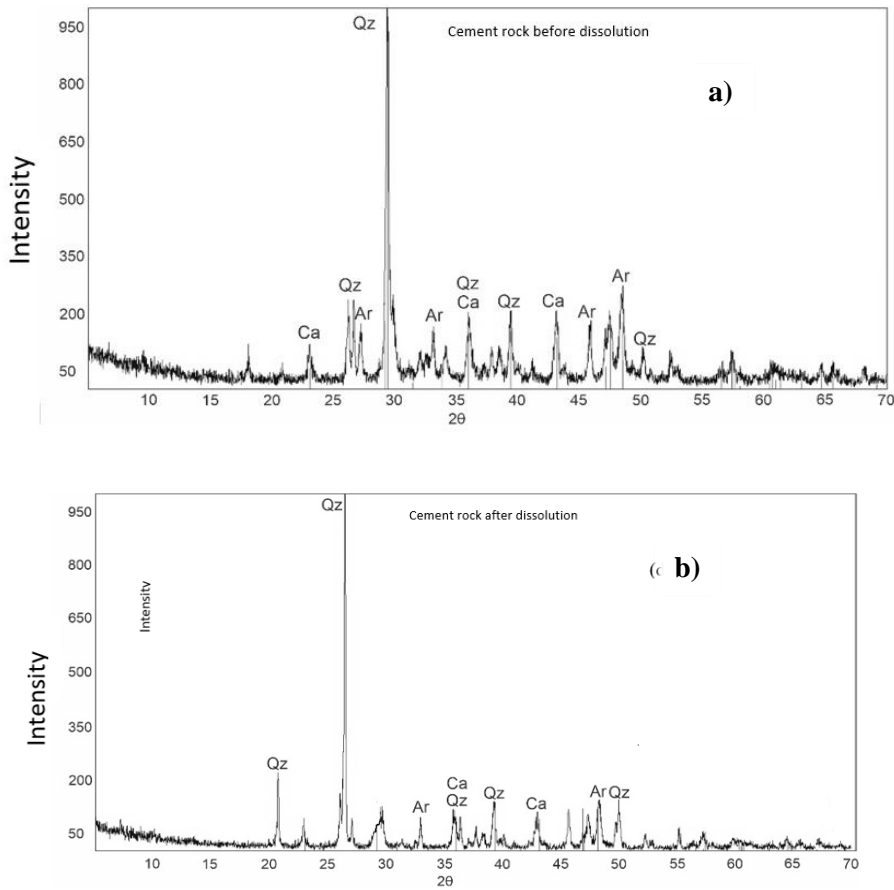


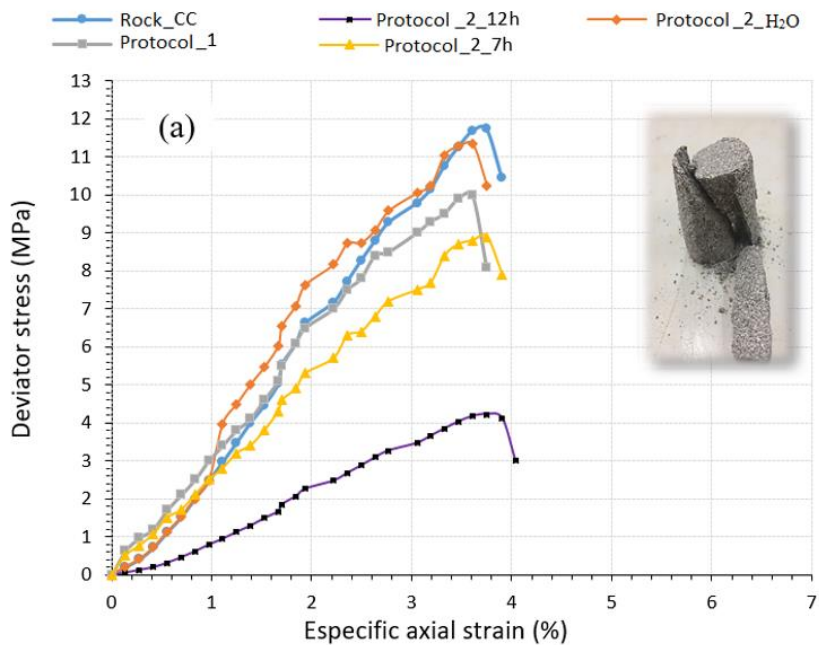
Figure 18: X-ray diffractogram of synthetic rock with cement (a) before dissolution and b) after sample dissolution

In the XRD (X-ray diffractogram) analysis, the minerals with higher solubility coefficients are seemingly more

conductive to dissolution since the minerals that make up the CH sample are more soluble and, therefore, more dissolved than those in the CC sample.

3.2.2 Mechanical Characteristics of samples before and after dissolution: Unconfined Compressive strength tests (UCS) and Brazilian testes

Figure 19 shows the results of the UCS tests, and Figure 20 shows the results of the Brazilian tests. The specific axial strain versus stress of rock samples is shown before and after the dissolution. As the samples were exposed to interaction with fluids, the peak stresses of uniaxial compression σ_c , of tensile σ_t , and Young's modulus E decreased significantly, especially in samples that have been exposed to the acid solution. Table 7 describes the results of UCS and tensile tests, including Young's modulus E of the rock samples and fluids. Before dissolution, the CH rock sample was more deformable than the CC sample, and the loss of strength due to compression and tensile are higher. Although the time of exposure to the fluid also influenced the dissolution of minerals, the pH of the solution accelerated the dissolution of these minerals considerably and changed the physical and mechanical characteristics of these samples. Figure 21 shows the relationship between UCS after and before dissolution (σ_c/σ_c before) versus the relationship between peak tensile strength after and before dissolution (σ_t/σ_t before). The effect of the dissolution process on the strength loss due to unconfined compression and tension is observed for the samples of Protocol 1 and 2 with the two fluids. The curve suggests that the rate of loss resistance to UCS and Brazilian test are related, and that loss of resistance is more evident in dissolutions with the acid solution, corroborating with the analysis of physical characteristics, which are also reflected in the mechanical characteristics of rock samples.



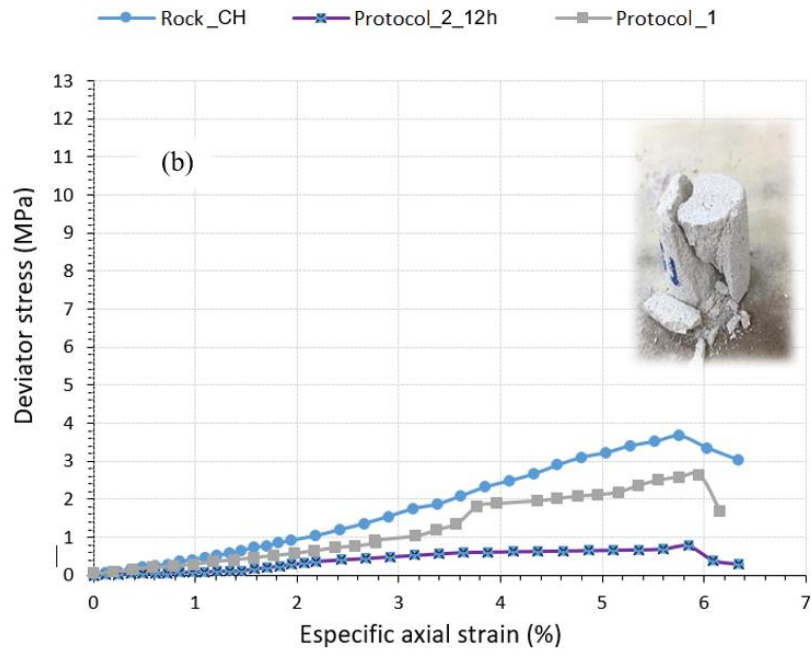
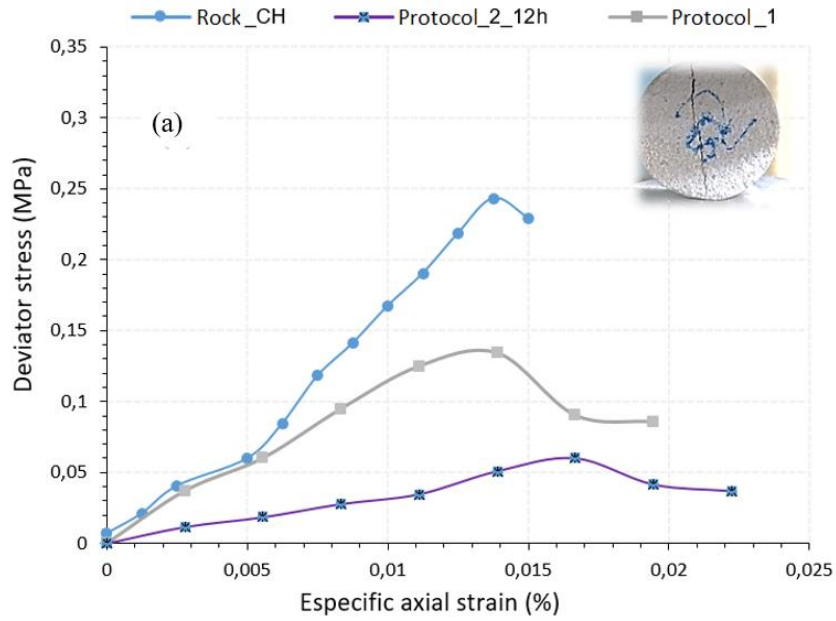


Figure 19: Stress versus strain curves of the unconfined compressive strength test—(a) calcium hydroxide sample (CH) and (b) cement sample (CC). Dissolution 1 refers to Protocol 1, and Dissolution 2 refers to Protocol 2.



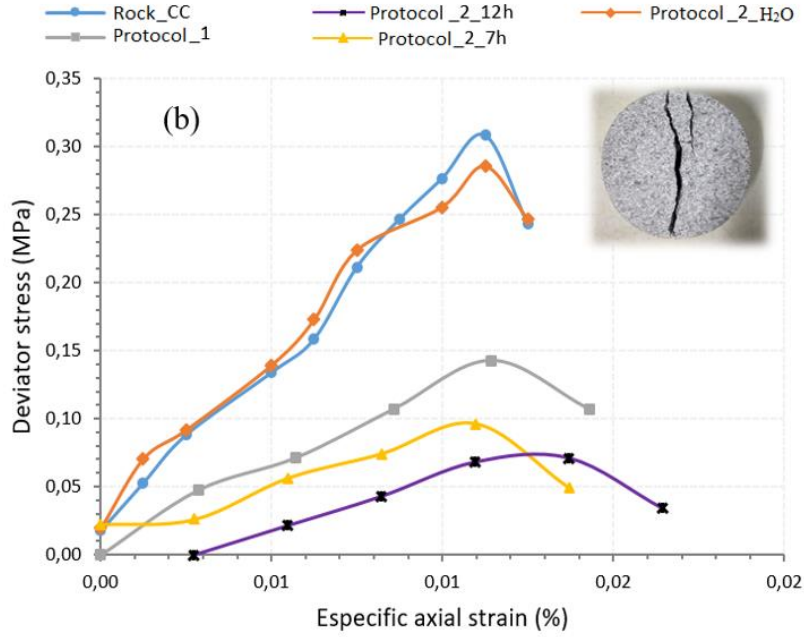


Figure 20: Stress versus strain curves of the Brazilian tests–(a) calcium hydroxide sample (CH) and (b) cement sample (CC). Dissolution 1 refers to Protocol 1, and Dissolution 2 refers to Protocol 2.

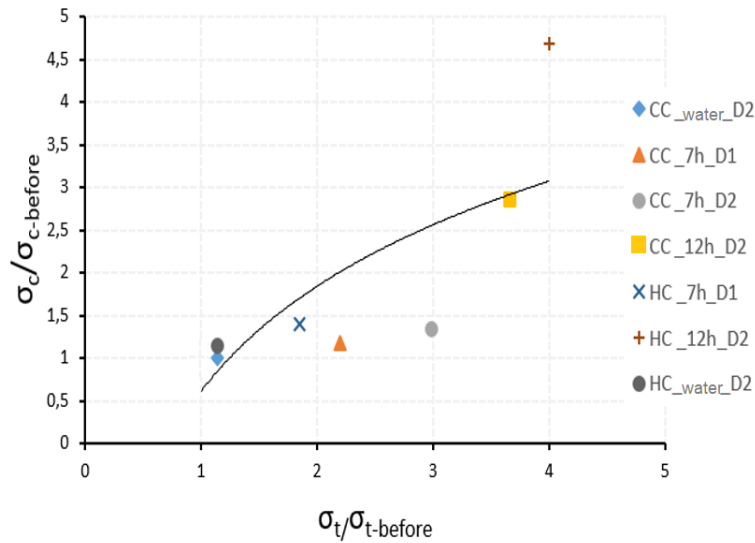


Figure 21: Relationship between UCS after and before dissolution versus the relationship between peak tensile strength after and before dissolution.

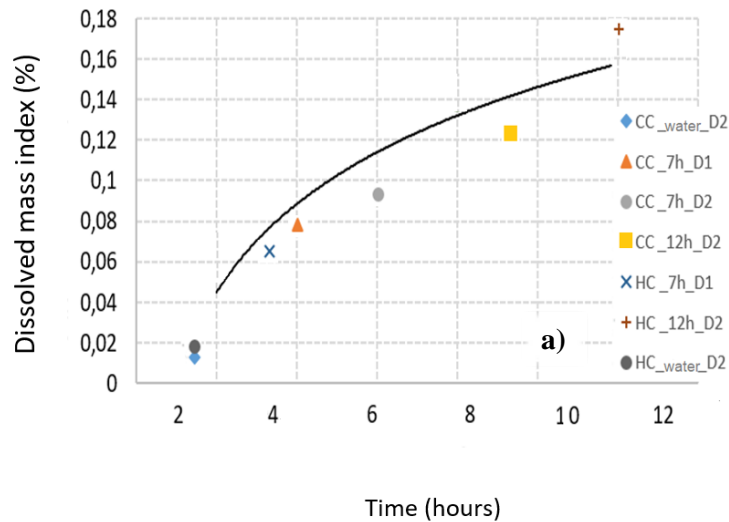
Minerals dissolution caused the loss of compressibility of roughly 78% for the CH samples and 65.1% in the CC samples. To understand the difference in the dissolution degree with solutions of different pH, the bonding forces that exist between the grains of these samples are taken into account. According to [13], considering the microstructure of the bonding, the grains can be subdivided into two classes: (1) diagenetic bondings of cementing material, which are strong connections formed during the production of samples, and (2) deposition

bondings, which are particles of the suspended cementing material, formed after the samples production, i.e., weaker bondings.

Table 7: Mechanical characteristics of samples before and after the dissolution test.

Samples	UCS σ_c (MPa)	σ_t (MPa)	E (GPa)
Calcium Hidroxido_Rock (before)	3,65	0,24	0,059
Protocol 1	2,62	0,13	0,041
Protocol 2	0,78	0,06	0,013
Protocol 2 water	3,20	0,21	0,052
Cement_Rock (before)	11,74	0,33	0,313
Protocol 1	10,00	0,15	0,256
Protocol 2 7h	8,80	0,11	0,223
Protocol 2 12h	4,10	0,09	0,103
Protocol 2 water	11,34	0,29	0,302

Therefore, in the tests with water flow, this material was carried in suspension because, despite obtaining a strain and a mass loss, their mechanical characteristics changed, as previously shown in the results. Figure 22a shows the time evolution of the dissolved mass index for all dissolution tests performed, and Figure 22b–c relates this mass loss that occurred in the dissolution with the loss of compressive and diametral strength normalized. The mass loss increased with the time of exposure of the rock with the fluid in the CH and CC samples. The test with water lost the least mass (Figure 22a). In Figure 22b–c, the dissolved mass index increases with time, and the normalized compressive strength of the rock samples decreases.



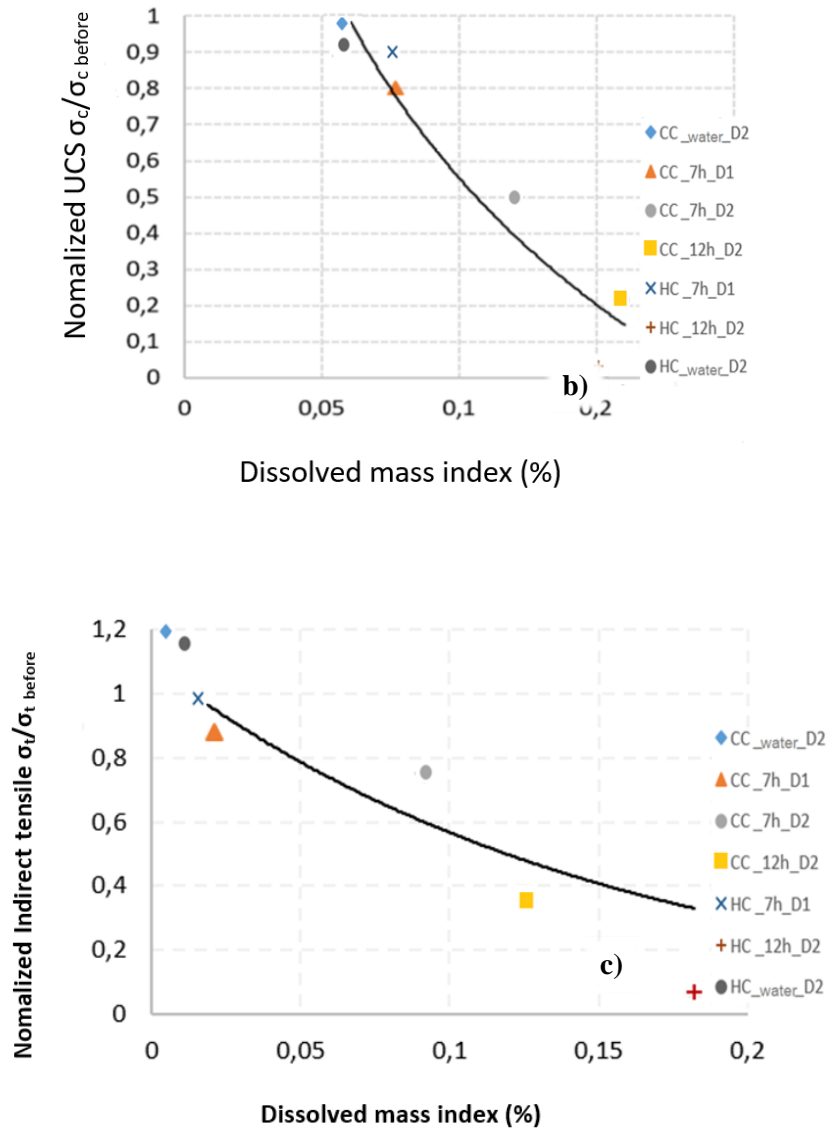


Figure 22: (a) Dissolved mass index over time and dissolved mass index vs. UCS (b) Brazilian (c) normalized compressive strength of synthetic rock samples with calcium hydroxide and cement.

The result of the chemical dissolution of diagenetic bonds takes place when calcarenite is flooded by the acid for a long period. With time, the bonds forming the structure of the soft rock are progressively weathered, tending the material to turn into a calcareous soil. The process evolution is governed by both the rate of the dissolution reaction and the ionic composition of the reactive fluid. The driving variable of the dissolution is the accumulated relative mass removal of calcite from the solid (or reaction progress) [26,25].

4. Conclusions

Through a study with synthetic rocks, this paper discussed how “soft” carbonate rocks transform when in contact with fluids. To assess the changes that occur in the physical and mechanical characteristics of carbonate rocks, two types of artificially cemented carbonate rocks with controlled physical and mechanical characteristics

were produced, and their behaviors were evaluated. In the rock samples, changes in their characteristics were observed, which were due to their components having a certain degree of solubility in water, and this degree is increased when in acid solution. Thus, the following was observed: Dissolution with the acid solution for longer fluid injection time caused the highest volumetric strains and effective horizontal stresses. In addition, as the material weakened from the dissolution, the effective horizontal stress gradually increased. The stress and strain analyses explain the influence the sample weakening phase has on the mechanical behavior of the samples at different dissolution times. As the rock lost its bondings, the elastic domain and the mechanical strength were affected. In protocol 3, the acid solution accelerated the mineral dissolution, owing to the reaction between H⁺ ion and calcite minerals. The interaction between the rock and fluid caused changes in the physical properties of the samples, such as increased porosity, by about 61.2% and 44.3% for the CH and CC samples, respectively. Considering the microstructure, this increase in porosity was due to the dissolution of calcite minerals, analyzed through petrographic analysis and XRD. These analyses also quantified the changes in the mechanical characteristics of the samples. The loss in maximum strength of the synthetic rocks studied was about 78% and 65% in the CH and CC samples, respectively. The studies developed with synthetic rocks can better quantify, represent, and explain the impacts in the mechanical, hydraulic, thermal, and chemical properties of rocks when in contact with a reactive fluid. These results with the modified oedometric cell provide insight into rock behavior because they reflect processes that occur when rocks come into contact with reactive fluids by acidification of the reservoir, advanced recovery of oil or gas, compaction and subsidence, pressure buildup, loss of wells due to collapse and reduction of shear stresses in the well wall. These incidents can lead to reactivating geological faults, thus inducing seismic events, which could cause irreversible damage to the rocks.

Acknowledgment

The authors acknowledge the financial support from PETROBRAS.

5. Recommendations

For future research, it is recommended to build an oedometric cell of more resistant material, for a longer period time of analyses and with more applications of vertical loads. Also, it is suggested to produce new carbonatic synthetic rocks, for physical and mechanical characterization.

References

- [1]. THOMAS, José Eduardo. Fundamentos de Engenharia de Petróleo. Rio de Janeiro: Ed Interciência, 2001.
- [2]. AHR, W. M. (2008) Summary: Geology of Carbonate Reservoirs, in Geology of Carbonate Reservoirs: The Identification, Description, and Characterization of Hydrocarbon Reservoirs in Carbonate Rocks, John Wiley & Sons, Inc., Hoboken, NJ, USA. doi: 10.1002/9780470370650.ch8.
- [3]. GUIMARÃES, L.J.N., GOMES, I.F., VALADARES, J.P. (2009). Influence of mechanical constitutive model on the coupled hydro-geomechanical analysis of fault reactivation. In: Reservoir Simulation Symposium - Society of Petroleum Engineers SPE, The Woodlands, 2-4 February 2009, SPE-119168-

PP. Texas: EUA.

- [4]. AUSTAD, T. et al (2008). Seawater in Chalk: An EOR and Compaction Fluid. Society of Petroleum Engineers. doi:10.2118/118431-PA.
- [5]. KORSNES, R.I.; MADLAND, M.V., VORLAND, K.A.N, HILDEBRAND-HABEL, T., KRISTIANSEN, T.G.;HIORTH, A. Enhanced Chemical Weakening of Chalk due to Injection of CO₂ Enriched Water. 29^o International Symposium of the Society of Core Analysts, Abu Dhabi. pp. 1-12, 2008.
- [6]. CIANTIA MO, CASTELLANZA R, DI PRISCO C (2015) Experimental study on the water-induced weakening of calcarenites. *Rock Mech Rock Eng* 48:441–461.
- [7]. TANG, Z. C., ZHANG, Q. Z., PENG, J., JIAO, Y. Y. Experimental study on the water-weakening shear behaviors of sandstone joints collected from the middle region of Yunnan province, P.R. China., *Engineering Geology*, Volume 258, 2019.
- [8]. YANG, F. ZHOU, H. ZHANG, C., JINGJING LU, LU, X. GENG, Y. An analysis method for evaluating the safety of pressure water conveyance tunnel in argillaceous sandstone under water-weakening conditions, *Tunnelling and Underground Space Technology*, Volume 97, 2020.
- [9]. SUGUIO, K. 2003. *Geologia Sedimentar*. Ed. Edgar Blücher Ltda.
- [10]. CASTELLANZA, R., and NOVA, R. (2004). “Oedometric tests on artificially weathered carbonatic soft rocks.” *J. Geotech. Geoenviron. Eng.*, 130(7).
- [11]. MERODO, F. J., et al., (2007). Coupling transport of chemical species and damage of bonded geomaterials. *Comp. & Geotechnics* 34(4). 200-215.
- [12]. SHIN, H., & SANTAMARINA, J. C. (2009). Mineral dissolution and the evolution of k₀. *Journal of Geotechnical and Geoenvironmental Engineering*, 135(8), 1141-1147.
- [13]. CIANTIA MO, HUECKEL T. (2013) Weathering of stressed submerged stressed calcarenites: chemo-mechanical coupling mechanisms. *Ge´otechnique* 63(9):768–785.
- [14]. VIEIRA, K. N. ; JESUS, L. L. ; LIMA, A. ; Guimaraes, L.J.N. (2017). Acid Dissolution Analysis of Artificial Carbonate Rock Cemented With Cp V - Ari. In: 9th Brazilian Congress of Research and Development in Oil and Gas, 2017, Maceió, 2017.
- [15]. VALLEJOS, J. A., SUZUKI, K., BRZOVIC, A., IVARS, D. M. Application of Synthetic Rock Mass modeling to veined core-size samples, *International Journal of Rock Mechanics and Mining Sciences*, Volume 81, 2016, Pages 47-61.

- [16]. FEDRIZZI, R. M. et al., (2018). Artificial carbonate rocks: Synthesis and petrophysical characterization. UENF, BRAZIL.
- [17]. NIRLAULA, L.D. Development of Modified T-z Curves for Large Diameter Piles/drilled Shafts in Limestone for Fb-pier. M.Sc. thesis University of Florida, Florida (2004), p. 163.
- [18]. ZHANG, X.; SPIERS, C. J. Compaction of granular calcite by pressure solution at room temperature and effects of pore fluid chemistry. *International Journal of Rock Mechanics & Mining Sciences*, v. 42, p. 950-960, 2005.
- [19]. SILVA, N.V.S. (2012). Capillary and Chemical Compaction Modeling in Oil Reservoirs. Doctoral thesis. Department of Civil Engineering, Federal University of Pernambuco, Pernambuco, Brazil, 122 p.
- [20]. MELO, L. M. P.; Leonardo José do N. Guimarães ; LINS, C. M. M. ; LIMA, A. Experimental numerical analysis of synthetic carbonate rock subjected to the injection of a reactive fluid. In: VIII Brazilian Symposium on Unsaturated Soils, 2015, Fortaleza. ÑSAT 2015 VIII Brazilian Symposium on Unsaturated Soils, 2015
- [21] LIMA NETO, I.A., R.M. MISSÁGIA, M.A. CEIA, N.L. ARCHILHA, AND L.C. OLIVEIRA, 2014, Carbonate pore system evaluation using the velocity-porosity–pressure (17) (PDF) Carbonate microporosity aspect ratio and -wave velocity prediction from 2D/3D digital image analysis, using inclusion theory. Relationship, digital image analysis, and differential effective medium theory: Elsevier, *Journal of Applied Geophysics* 110, 23-33. doi:10.1016/j.jappgeo.2014.08.013.
- [22]. LINS, C.M.M.S, GUIMARÃES, L., LIMA A., GOMES, I. (2015) Numerical and Experimental Analysis of Horizontal Stress Changes and Soil Collapse During Chemical Dissolution in a Modified Oedometer Cell. *International Journal of Geotechnical and Geoenvironmental Engineering, Soils and Rocks*. V.39, n. 1, p 4-12, January 2015.
- [23] NBR- ANBT- 12025/12. Ensaio de compressão simples de corpos de prova cilíndricos- Método de ensaio.
- [24]. SCHOLLE, P.A. & ULMER-SCHOLLE, D.S (2003)., A Color Guide to the Petrography of Carbonate Rocks, Grains, Textures, Porosity, Diagenesis, AAPG Memoir 77, P. 212.
- [25]. CIANTIA, M.O., CASTELLANZA, R., DI PRISCO, C., 2014. Experimental study on the water-induced weakening of calcarenites. *Rock Mech. Rock. Eng.* <http://dx.doi.org/10.1007/s00603-014-0603-z>
- [26]. De Groot SR (1966) *Thermodynamics of irreversible processes*. Amsterdam, North Holland.